J Mater Sci (2009) 44:4460–4465
DOI 10.1007/s10853-009-3676-4

Effects of metal oxides addition on the electrochemical performance of $M1Ni_{3.5}Co_{0.6}Mn_{0.4}Al_{0.5}$ hydrogen storage alloy

Hongxia Huang · Kelong Huang · Suqin Liu · Shuxin Zhuang · Dongyang Chen

Received: 8 April 2009 / Accepted: 9 June 2009 / Published online: 27 June 2009

Abstract The AB_5-type $M1Ni_{3.5}Co_{0.6}Mn_{0.4}Al_{0.5}$ alloy (where M1 denotes mixed lanthanide) was modified with different additives (ZnO and MnO_2), and the effects of metal oxides on the electrochemical properties of the $M1Ni_{3.5}Co_{0.6}Mn_{0.4}Al_{0.5} - x\%$ M ($x = 5$, 10; M = ZnO, MnO_2) alloy were studied. The results showed that the addition of metal oxides had a positive effect on the activation property of the alloy electrode. With the addition of ZnO, the maximum discharge capacity of the alloy increased from 315 to 334 mAh/g ($x = 5$) and 341 mAh/g ($x = 10$) with good cycle capability (C_{30}/C_{max}) (87% for $x = 5$ and 85% for $x = 10$), while the maximum discharge capacity remained invariable and the cyclic stability was deteriorated by the addition of MnO_2. Linear polarization (LP), cycle voltammetry (CV), and electrochemical impedance spectroscopy (EIS) measurements were also performed to investigate the electrochemical kinetics of alloy electrodes.

Introduction

$LaNi_5$-type rare earth-based alloys have been paid much attention due to their high capacity, high charge/discharge ability, ease of activation, and low hydriding/dehydriding pressure. However, the currently commercialized AB_5-type electrode alloys cannot meet the demand of the powder battery owing to the limitation of its low discharge capacity. It still has a large distance to 372 mAh/g of $LaNi_5$ theoretical capacity. To exploit the potential capacity of AB_5-type alloy, a lot of investigations have been carried out: (1) substitution of alloy elements [1–5]; (2) surface treatment [6–8]; (3) elaboration of alloy composite [9–11]; (4) powder sieving [12]; and (5) control of the charge input [13]. Among them, adding the 3d transition metal oxides into alloy electrodes is a simple and low production cost method to improve the electrochemical properties. For example, Khrussanova and Oelerich [14, 15] revealed that the hydriding/dehydriding kinetics of hydrogen storage alloys was improved with the addition of the oxides of the 3d transition metals such as TiO_2, Cr_2O_3, V_2O_5, MnO_2, Fe_3O_4, CuO, and Al_2O_3. Iwakura et al. [16, 17] reported that the discharge capacity of $MmNi_{3.6}Mn_{0.4}Al_{0.3}Co_{0.7}$ alloy was enhanced by addition of RuO_2 and Co_3O_4. Cheng et al. [18] observed that the electrochemical performances of AB_5-type alloys were improved significantly by mixing it with Bi_2O_3 and CuO. Cui and Luo [19] found the discharge capacity and high- rate dischargeability (HRD) of $Mg_{1.9}Y_{0.1}Ni_{0.9}Al_{0.1}$ alloy were greatly increased by the modification with the oxide addition (RuO_2, Ag_2O, Fe_2O_3, MoO_3, and V_2O_5). Wang et al. [20] reported that the electrochemical properties of the nanocrystalline $LaMg_{12}$-Ni were improved by modifying with a small amount of TiO_2 and Fe_3O_4. Zhang et al. [21] studied the catalytic effect of metal oxides (Fe_2O_3, TiO_2, Cr_2O_3, and ZnO) addition on the electrochemical properties of the $La_{1.3}CaMg_{0.7}Ni_9$ hydrogen storage alloy and found that not only the discharge capacity but also the high-rate dischargeability is improved by addition of 5 wt% TiO_2, Cr_2O_3, and ZnO. Although some important progresses have

H. Huang · K. Huang (✉) · S. Liu · S. Zhuang · D. Chen
College of Chemistry and Chemical Engineering, Central South University, Changsha 410083, People's Republic of China
e-mail: huangkelong@yahoo.com.cn

H. Huang
The Department of Material and Chemistry, Guilin University of Technology, Guilin 541004, People's Republic of China
e-mail: hhxhunan@yahoo.com.cn

been obtained, none of the currently commercialized $LaNi_5$ alloys can meet the demand of power battery. A simple and low production cost method is adding the 3d transition metal oxides into alloy electrodes to further improve the overall electrochemical properties of $LaNi_5$-type rare earth-based alloys.

In this work, the $LaNi_5$-based $M1Ni_{3.5}Co_{0.6}Mn_{0.4}Al_{0.5}$ alloy was modified with different contents of ZnO and MnO_2. The effect of addition of metal oxides on the microstructure, the activation property, the electrochemical discharge capacity, and cycle stability of the $M1Ni_{3.5}Co_{0.6}Mn_{0.4}Al_{0.5}$ alloy was systematically investigated in order to evaluate the potential of this type alloy as hydride electrodes in Ni/MH batteries.

Experimental

The $M1Ni_{3.5}Co_{0.6}Mn_{0.4}Al_{0.5}$ alloy (M1 consists of 37.7% La, 38.9% Ce, 6.3% Pr, and 17.1% Nd) was prepared by induction melting under argon atmosphere and remelted four times for homogeneity. The purity of all the constituent metal elements was over 99.0%. The $M1Ni_{3.5}Co_{0.6}Mn_{0.4}Al_{0.5}$ ingots were mechanically crushed to powders. Part of the crushed power was milled for 0.5 h, and then sieved to 300 meshes for XRD analysis and electrochemical test. The oxide-modified alloys were prepared by ball milling of the crushed power with $x\%$ M ($x = 5$, 10; M = ZnO, MnO_2), then ground by planetary ball miller under argon atmosphere for 0.5 h, the ball to powder weight ratio was 20:1. The alloy powders were sieved to 300 meshes for test.

The structures of the alloys were measured by powder X-ray diffraction (Japan D/max 2550 VB + 18 kV diffractometer) using Cu K_α radiation ($\lambda = 1.54178$ Å).

The working electrodes for electrochemical measurements were fabricated by mixing 100 mg alloy powder with 200 mg carbonyl nickel powder. The mixture was then pressed into a pellet of 10 mm in diameter under a pressure of 10 MPa. Both sides of the electrode pellet were coated with two foamed nickel sheets, then pressed at 30 MPa, and tightly spot-welded. Electrochemical measurements were performed in a standard open two-electrode electrolysis cell consisting of a working electrode (the MH electrode), a sintered $Ni(OH)_2$/NiOOH counter electrode, and 6 mol/L of KOH solution as electrolyte. Charge/discharge cycles were conducted by an automatic LAND 5.3 B battery test instrument. The voltage between the negative electrode and the reference electrode was defined as the discharge voltage. The electrodes were charged for 6 h at a current density of 100 mA/g, rested for 5 min, and then discharged to the cut-off potential of 0.8 V at a current density of 50 mA/g.

During EIS, linear polarization and Tafel polarization tests, HgO/Hg electrode was used as reference electrode. CHI 660 C electrochemical workstation was used for CV measurement (scanning rate: 0.1 mV/s, potential range: −1.2 to −0.2 V vs. HgO/Hg); Tafel polarization (scanning rate: 1 mV/s, potential range: −1.0 to −0.2 V vs. HgO/Hg); linear polarization (scanning rate: 0.1 mV/s, −5 to 5 mV vs. open circuit potential), and EIS (potential: −0.85 V, amplitude: 5 mV, frequency range: 1×10^3 Hz–1×10^{-3} Hz). All the experiments were conducted at room temperature.

Results and discussions

X-ray diffraction patterns (XRD)

Figure 1 presents the XRD patterns of the $M1Ni_{3.5}Co_{0.6}Mn_{0.4}Al_{0.5} - x\%$ M ($x = 5$, 10; M = ZnO, MnO_2). The pristine alloy consists of single hexagonal $CaCu_5$-type $LaNi_5$ phase in space group *P6*/mmm. Comparing with XRD pattern of the pristine alloy, the diffraction peaks of ZnO and MnO_2 obviously appear in the modified alloys. It can be concluded that the metal oxide particles can be easily dispersed onto the particles of $LaNi_5$-type alloy powders during ball milling.

Activation capability and discharge capacity

Figure 2 shows the cycle number dependence of the discharge capacity of the $M1Ni_{3.5}Co_{0.6}Mn_{0.4}Al_{0.5}$ alloy modified with metal oxides. An outstanding characteristic from a commercial point of view is that the composite electrodes can be activated in two cycles, so an extended

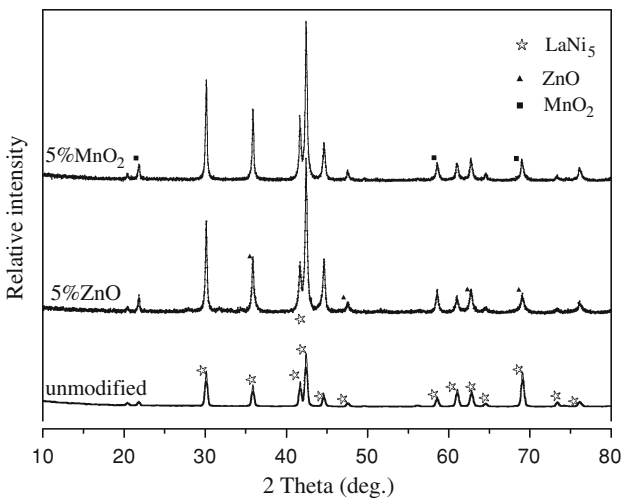

Fig. 1 XRD patterns of $M1Ni_{3.5}Co_{0.6}Mn_{0.4}Al_{0.5}$ alloy modified with different metal oxides

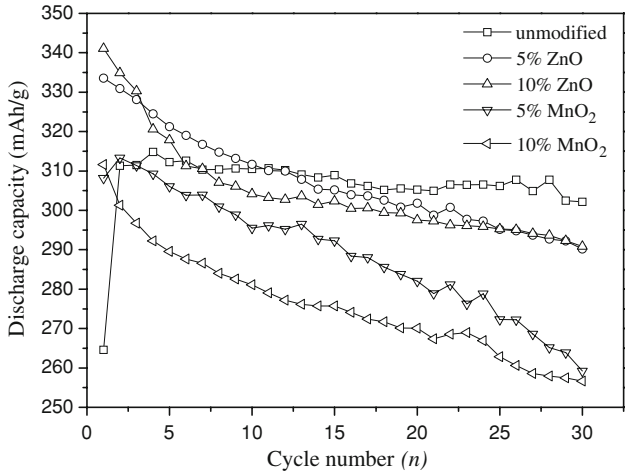

Fig. 2 The discharge capacity of $M1Ni_{3.5}Co_{0.6}Mn_{0.4}Al_{0.5}$ electrodes modified with different metal oxides as a function of cycle number

period of activation process is unnecessary as it is the case for other alloy electrodes. This result suggests that it is possible to improve the activation property of the alloy electrode by a small amount of metal oxide addition. The activation capability of the alloy is related to the phase structure, surface state, grain size, composition homogeneity, and interstitial dimensions of the alloy [22]. It is accepted that the smaller the additive strain energy, which is inevitable when the hydrogen atoms enter the interstitial of the tetrahedron or octahedron of the alloy lattice, the better is the activation performance of the alloy [23]. One explanation may be offered as the reasons why the addition of metal oxides enhances the activation characteristic of the alloy. During the process of ball milling, the particles of ZnO and MnO_2 can be easily cohered onto the large $LaNi_5$-type alloy powders during ball milling. The small particles of metal oxides have an electro-catalytic effect and can improve the activation performance of the pristine $M1Ni_{3.5}Co_{0.6}Mn_{0.4}Al_{0.5}$ alloy electrode.

The results in Fig. 2 indicate that modification of the $M1Ni_{3.5}Co_{0.6}Mn_{0.4}Al_{0.5}$ alloy with ZnO results in an increment of the maximum discharge capacity, while MnO_2 addition causes an unfavorable effect. After addition with ZnO, the maximum discharge capacity of $M1Ni_{3.5}Co_{0.6}Mn_{0.4}Al_{0.5}$ alloy increased from 315 to 334 mAh/g ($x = 5$) and 341 mAh/g ($x = 10$). After 30 cycles, the discharge capacity for alloy electrodes modified with ZnO are 290 mAh/g ($x = 5$) and 291 mAh/g ($x = 10$), and the cycle capability (C_{30}/C_{max}) is 87% for $x = 5$ and 85% for $x = 10$, respectively. Contrarily, the addition of MnO_2 in this experiment has no significant influence on the discharge capacity. Further, it is noteworthy that the alloys modified with metal oxides show quick capacity decay compared with unmodified $M1Ni_{3.5}Co_{0.6}Mn_{0.4}Al_{0.5}$ alloy. It is presumed that the oxide addition probably increases the surface oxidation of alloy during charging and discharge, resulting in poor cycle stability.

Discharge potential characteristic

Generally, the plateau potential is related to the internal resistance of the battery, including ohmic resistance and polarization resistance. The electrode with higher discharge potential and lower charge potential means that the internal resistance is small. The longer and more horizontal the discharge potential plateau is, the better would be the discharge performance of the alloy electrode. Figure 3 shows the discharge potential curves of alloy electrodes. In the order of 10% MnO_2 < 5% MnO_2 < unmodified < 5% ZnO < 10% ZnO, the discharge curve becomes more horizontal. Thus, the effect of addition of 10% ZnO on discharge property of alloy electrode is significant. Khrussaova et al. [24] revealed that during mechanical alloying and hydriding, the 3d transition metal oxides were partial reduced to clusters of the corresponding transition metal, which facilitated the dissociative hydrogen chemisorption and improved the hydriding/dehydriding.

Linear polarization (LP)

Figure 4 shows the linear polarization curves of $M1Ni_{3.5}Co_{0.6}Mn_{0.4}Al_{0.5} - x\%$ M ($x = 5$, 10; M = ZnO, MnO_2) alloy electrodes. The exchange current density (I_0) is an important kinetic parameter, which can be used to estimate the kinetic property of the electrochemical hydrogen reaction at the equilibrium state and indicates the reaction rate of hydrogen on the alloy surface [25]. As shown in Fig. 4, there is a good linear dependence between the current density and the overpotential within a small interval. According to the slope of linear polarization patterns,

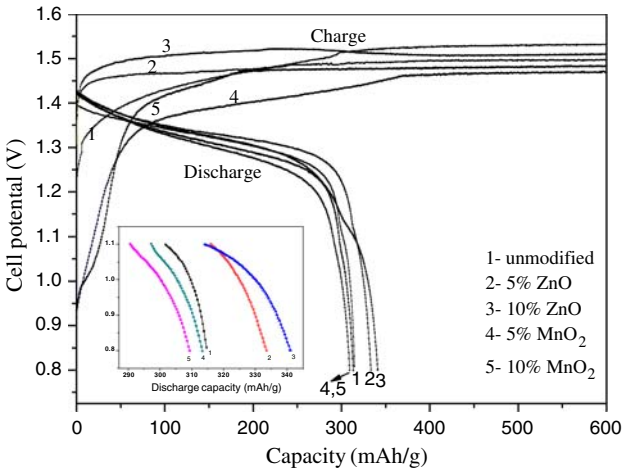

Fig. 3 Discharge curves of the $M1Ni_{3.5}Co_{0.6}Mn_{0.4}Al_{0.5}$ alloy modified with different contents of ZnO and MnO_2

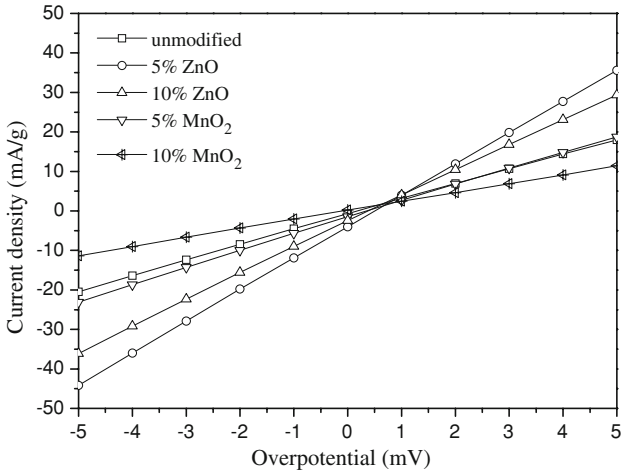

Fig. 4 Linear polarization curves of alloy electrodes modified with different metal oxides

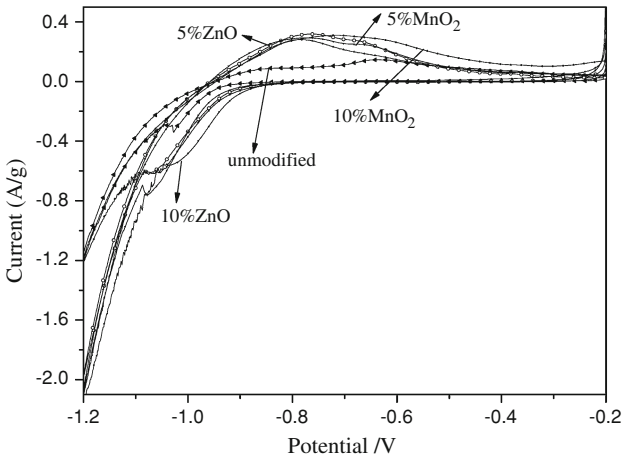

Fig. 5 CV curves for alloy electrodes modified with different metal oxides at a scanning speed of 0.1 mV/s

the polarization resistance (R_p) can be obtained. I_0 is calculated according to the following formula [24]:

$$I_0 = \frac{RTI_d}{F\eta} \quad (1)$$

where R is the gas constant, T is absolute temperature, I_d is applied current density, F is Faraday constant, and η is the overpotential. The R_p values and I_0 of alloy electrodes are listed in Table 1. The R_p increases from 123 to 500 mΩ in the order of 5% ZnO < 10% ZnO < 5% MnO_2 < unmodified < 10% MnO_2 and the exchange current density I_0 decreases from 205 to 51 mA/g. This result confirms that the kinetic property of the electrochemical hydrogen reaction of $M1Ni_{3.5}Co_{0.6}Mn_{0.4}Al_{0.5}$ electrode is improved by modifying with 5% ZnO, 10% ZnO, and 5% MnO_2, so the overpotential is reduced during the process of charge/discharge. It can be suggested that ZnO can act as a good catalyst and provide more active sites on the alloy surface, facilitating the charge transfer on the surface of the alloy and the diffusion of hydrogen atoms from the surface to the inside of the alloy, which enhances the dynamical property of alloy in the process of hydrogen absorption and desorption. But excessive MnO_2 exerts a negative effect on the electrocatalytic activity for hydrogen electrode reaction. Generally, the alloy electrode with addition of 5% ZnO has the best electrochemical hydrogen absorb/desorb kinetics.

Cyclic voltammograms (CV)

Figure 5 shows the CV curves of $M1Ni_{3.5}Co_{0.6}Mn_{0.4}Al_{0.5} - x\%$ M ($x = 5$, 10; M = ZnO, MnO_2) at the potential interval of −1.2 to −0.2 V vs. HgO/Hg. The anodic peak at around −0.8 V vs. HgO/Hg is attributed to the oxidation of hydrogen absorbed in the alloy according to the following equation [26]:

$$MH_n + nOH^- \rightarrow M + nH_2O + ne^- \quad (2)$$

The cathodic peak at around −1.0 to −1.1 V vs. HgO/Hg is attributed to the hydriding according to above equation at opposite side. The anodic peak current can be used to evaluate the kinetics of hydrogen oxidation reaction on the interface of alloy and the discharge capacity can be calculated according the peak area [27]. As seen in Fig. 5, the reduction current density peak for $M1Ni_{3.5}Co_{0.6}Mn_{0.4}Al_{0.5}$ does not appear in the investigated potential range. It indicates that absorption of hydrogen occurs only at limited active sites on the $M1Ni_{3.5}Co_{0.6}Mn_{0.4}Al_{0.5}$ alloy surface, which is attributed to the loss of active sites due to the formation of a dense oxide layer on the surface, which baffles the adsorption of hydrogen on the surface and hydrogen diffusion into the bulk of alloys. On the other hand, for the $M1Ni_{3.5}Co_{0.6}Mn_{0.4}Al_{0.5}$ alloy electrodes modified with different metal oxides, there are apparent reduction peaks at around −1.0 to −1.1 V vs. HgO/Hg. It can be concluded that the absorption and desorption of

Table 1 The polarization resistance (R_p) and exchange current density (I_0) for alloy electrodes

Samples	$M1Ni_{3.5}Co_{0.6}Mn_{0.4}Al_{0.5}$	5% ZnO	10% ZnO	5% MnO_2	10% MnO_2
R_p (mΩ)	333	123	161	294	500
I_0 (mA/g)	76	205	157	86	51

hydrogen in the alloy are remarkably improved and the active sites on the surface are greatly incremented after surface modification with metal oxides.

Electrochemical impedance spectra (EIS)

The electrochemical impedance spectra of $M1Ni_{3.5}Co_{0.6}Mn_{0.4}Al_{0.5}$ alloy modified with metal oxides at −0.85 V (vs. HgO/Hg) are shown in Fig. 6. It can be seen that each spectrum consists of a small semicircle in the high-frequency region and a large semicircle in the low-frequency region followed by a straight line. Kuriyama et al. [28] ascribed the high-frequency semicircle to the contact resistance between the current collector and the alloy pellet, the low-frequency semicircle to the charge-transfer resistance, and the straight line at low-frequency results from the Warburg impedance. As can be seen from Fig. 6 that the large semicircles in the low-frequency region for electrochemical reaction resistance are different for alloy electrodes, the R_{ct} is 5% ZnO < 10% ZnO < 5% MnO_2 < unmodified < 10% MnO_2, which is consistent with the result of R_p in Table 1. The above results indicate that the electrochemical reaction resistance changes reversely with the value of I_0.

Potentiodynamic polarization

Many efforts have been made to improve the anti-corrosion performance of alloy electrodes in alkaline solution, because the corrosion is a barrier to its practical application. Figure 7 shows the potentiodynamic polarization curves for the $M1Ni_{3.5}Co_{0.6}Mn_{0.4}Al_{0.5}$ alloy electrodes modified with metal oxides. The larger of the corrosion voltage (E_{corr}) means the better anti-corrosion performance

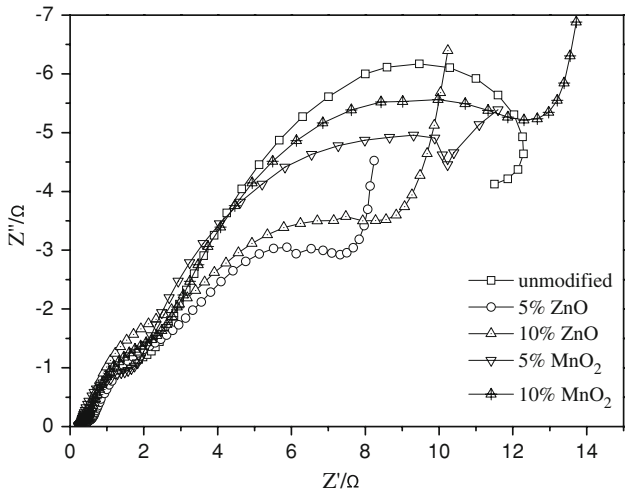

Fig. 6 The electrochemical impedance spectra (EIS) of electrodes modified with different metal oxides at value of −0.85 V

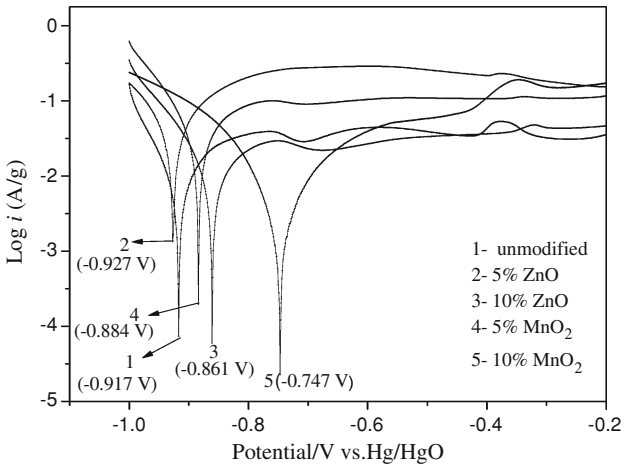

Fig. 7 Potentiodynamic polarization curves of alloy electrodes modified with different metal oxides

of the alloy. The values of corrosion voltage (E_{corr}) obtained through Tafel fitting are indicated in Fig. 7. It can be seen that the corrosion resistance of alloy electrode is in the order of 5% ZnO < unmodified < 5% MnO_2 < 10% ZnO<10% MnO_2. Excessive MnO_2 acts as a passive layer on the alloy surface, which increases the charge-transfer reaction resistance and baffles the diffusion of H atoms from the surface to the bulk of the alloy. The variation of corrosion voltage is not completely consistent with that of the cycle stability shown in Fig. 2. It reveals that the inhibition of metal corrosion is not always the main factor for the improvement of cycle performance of alloy.

Our result is different from Oelerich's result [15], which reported that only the metal oxides having different valences could play an important role on the kinetics of the hydrogen absorption and desorption of nanocrystalline MgH_2, but the oxides such as Al_2O_3, SiO_2, and Sc_2O_3, in which the metal atom appears with only a single valence state have no catalytic effect. In the present study, the alloy electrode with addition of 5% ZnO shows the best electrochemical hydrogen absorb/desorb kinetics among the investigated electrodes, and a similar result was obtained by Zhang et al. [21].

According to the above analyses, it can be concluded that ZnO can serve as a microcurrent collector and electrocatalyst, which leads to an increase of the electrical conductivity and a reduction in the internal electric resistance, so the discharge capacity is increased by the addition of ZnO.

Conclusion

$M1Ni_{3.5}Co_{0.6}Mn_{0.4}Al_{0.5}$ composite alloys were prepared by ball-milling the pristine alloy and metal oxides (ZnO and

MnO_2); the electrochemical hydrogen storage properties of alloys were studied.

The activation property of the alloy electrode is improved by addition of metal oxides, and the maximum discharge capacity of $M1Ni_{3.5}Co_{0.6}Mn_{0.4}Al_{0.5}$ alloy is increased up from 315 to 334 mAh/g ($x = 5$) and 341 mAh/g ($x = 10$) with the addition of ZnO. The exchange current density I_0 decreased from 205 to 51 mA/g in the order of 5% ZnO > 10% ZnO > 5% MnO_2 > unmodified > 10% MnO_2, which indicates that the kinetic property of the $M1Ni_{3.5}Co_{0.6}Mn_{0.4}Al_{0.5}$ electrodes is improved by modifying with 5% ZnO, 10% ZnO, and 5% MnO_2, but excessive MnO_2 has a negative effect on the dynamical property of alloy. EIS analysis shows that the R_{ct} value is in the order of 5% ZnO < 10% ZnO < 5% MnO_2 < unmodified < 10% MnO_2, which agrees with the result of R_p.

Acknowledgement The authors wish to express their thanks to the National Natural Science Foundation of China (50772133) and the Open Subject of State of Key Laboratory for Powder Metallurgy of Central South University (2008112009).

References

1. Wang MH, Zhang LZ, Zhang Y, Sun LX, Tan ZC, Xu F, Yuan HT, Zhang T (2006) Int J Hydrogen Energy 31:775
2. Goo NH, Lee KS (2002) Int J Hydrogen Energy 27:433
3. Feng Y, Jiao LF, Yuan HT, Zhao M (2007) Int J Hydrogen Energy 32:1701
4. Liu YF, Pan HG, Gao MX, Miao H, Lei YQ, Wang QD (2008) Int J Hydrogen Energy 33:124
5. Zhang YH, Zhao DL, Li BW, Ren HP, Guo SH, Wang XL (2007) J Mater Sci 42:8172. doi:10.1007/s10853-007-1689-4
6. Souza EC, Ticianelli EA (2007) Int J Hydrogen Energy 32:4917
7. Liu FJ, Suda S (1996) J Alloys Compd 232:212
8. Hatano YJ, Tachikawa T, Mu D, Abe T, Watanabe K, Morozumi S (2002) J Alloys Compd 330–332:816
9. Wang Y, Qiao SZ, Wang X (2008) Int J Hydrogen Energy 33:1023
10. Pal K (1997) J Mater Sci 32:5177. doi:10.1023/A:1018633920700
11. Gao Y, Zeng MQ, Li BL, Zhu M (2003) J Mater Sci 38:2499. doi:10.1023/A:1023921605728
12. Rongeat C, Grosjean MH, Ruggeri S, Dehmas M, Bourlot S, Marcotte S, Rou′e L (2006) J Power Sources 158:747
13. Ruggeri S, Roue L (2003) J Power Sources 117:260
14. Khrussanova M, Peshev P, Ivanov EY, Terzieva M (1987) Mater Res Bull 22:405
15. Oelerich W, Klassen T, Bormann R (2001) J Alloys Compd 315:237
16. Iwakura C, Fukumoto Y, Matsuoka M, Kohno T, Shinmou K (1993) J Alloys Compd 192:152
17. Iwakura C, Matsuoka M, Kohno T (1994) J Electrochem Soc 141:2306
18. Cheng SA, Lei YQ, Leng YJ, Wang QD (1998) J Alloys Compd 264:104
19. Cui N, Luo JL (1998) Electrochim Acta 44:711
20. Wang Y, Gao XP, Lu ZW, Hu WK, Zhou Z, Qu JQ (2005) Electrochim Acta 50:2187
21. Zhang P, Wei XD, Liu YN, Zhu JW, Yu G (2008) Int J Hydrogen Energy 33:1304
22. Zhang YH, Li BW, Ren HP, Cai Y, Dong XP, Wang XL (2007) Int J Hydrogen Energy 32:3420
23. Zhang YH, Li BW, Ren HP, Cai Y, Dong XP, Wang XL (2007) Int J Hydrogen Energy 32:4627
24. Khrussanova M, Terzieva M, Peshev P (1991) Int J Hydrogen Energy 16:265
25. Notten PHL, Hokkeling P (1991) J Electrochem Soc 138:1877
26. Chen Y (1998) Catal Today 44:3
27. Liu YF, Pan HG, Gao MX, Li R, Gao MX (2004) J Alloys Compd 376:304
28. Kuriyama N, Sakai T, Miyamura H, Uehara I, Ishikawa H, Iwasaki T (1992) J Electrochem Soc 139:L72